Semicond. Sci. Technol. **12** (1997) 1187–1194. Printed in the UK PII: S0268-1242(97)84071-0

Effects of radiation damage in silicon p–i–n photodiodes

M McPherson†, B K Jones and T Sloan

School of Physics and Chemistry, Lancaster University, Lancaster LA1 4YB, UK

Received 6 May 1997, accepted for publication 10 July 1997

Abstract. The effects of radiation damage in two silicon p–i–n photodiodes fabricated from high resistivity material have been studied. The devices have been irradiated by 1 MeV neutrons to three different fluences up to 2.5×10^{14} n cm^{-2}. Current, capacitance and charge measurements were performed prior to irradiation and soon after. Our results indicate that the damage has degraded the charge-collection efficiency, that the devices have undergone type inversion from n-type to apparent p-type at fluences as low as 3×10^{13} n cm^{-2}, and that the substrate material has become somewhat 'relaxation-like' after irradiation. It is suggested here that irradiated silicon is relaxation material.

1. Introduction

In recent years a number of semiconductor materials have been investigated for use as radiation detectors in particle colliders. These include gallium arsenide (GaAs), which has been thought to be the best candidate but is not very well understood, and silicon (Si), which has been extensively researched and is fairly well understood. GaAs has good stopping power for x-rays and is radiation hard, while Si suffers from extensive radiation damage, the immediate effect being an increase in the reverse bias leakage current. Extensive work is being carried out at present to attempt to transform silicon into a radiation-hard semiconductor, and it is with this aim in mind that this current work was carried out. In this paper we report on the results. We also venture a conclusion that one of the main effects of radiation damage in silicon is to transform the substrate into relaxation material.

Neutron damage in a semiconductor is caused by collisions with nuclei within the bulk of the substrate material. The neutron is an uncharged particle, which means that the incident particles tend to be involved in the destruction of the host lattice. The lattice destruction introduces deep level defects that alter the electrical properties of the material. The defects so introduced are found to increase the resistivity of a semiconductor material, and are thus responsible for the semi-insulating behaviour, which has been attributed [1–3] to the relaxation-like properties in semiconductors. Relaxation materials are high resistivity due to a low carrier density, or are highly recombinative due to a high density of recombination centres. Neutron damage in the silicon material induces these two conditions, causing silicon to become relaxation-like.

† E-mail address: M.McPherson@lancaster.ac.uk

In the analysis assuming conventional lifetime material, the total current flowing in a diode can be expressed in terms of the series resistance R_s, the ideality factor η and the reverse saturation current I_s as

$$I = I_s \left[\exp\left(\frac{e(V - IR_s)}{\eta kT} \right) - 1 \right] \tag{1}$$

where V is the voltage across the diode, I is the current through the diode and k and e have their usual meaning. Here, the semiconductor is very pure with few defects and so has a good conductivity. Carriers flow easily to quickly neutralize any non-equilibrium space charge. Charge neutrality is thus always assumed in the depletion region, and so minority carrier injection induces majority carrier enhancement.

In the case of relaxation material, the current varies in a different manner. In this case, the diode is governed by space charge effects and the current assumes an ohmic variation in both bias directions. Here, the basic equilibrium condition is local zero net recombination or generation rate, such that $np - n_i^2 = 0$, which implies that the two types of carriers have the same Fermi energy level. The maximum resistivity thus occurs when this Fermi level is pinned at the location for minimum conductivity (or at midgap), and is given by the relation

$$\rho_{\max} = \frac{1}{2e(\mu_n \mu_p)^{1/2} n_i} \tag{2}$$

where μ_n and μ_p are the electron and hole mobilities respectively, and n_i is the intrinsic carrier concentration. Here, the rate at which charge is neutralized by carrier flow is slower than the generation rate of carriers by deep-lying generation–recombination centres. The dielectric relaxation time is the time in which a space charge is neutralized by the flow of free carriers drawn in by the charge but

slowed down by the resistance. It is related to the maximum resistivity as in the relation

$$\tau_D = \rho_{\max}\varepsilon_r\varepsilon_0 \tag{3}$$

where ε_r is the relative dielectric constant of the semiconductor material, and ε_0 is the dielectric constant of free space. The time in which excess minority carriers become annihilated by recombining with those of the opposite charge is the minority carrier recombination lifetime, τ_0. In this situation the condition for relaxation materials [4–6] is one in which $\tau_0 \ll \tau_D$, in contrast to the lifetime situation given by $\tau_0 \gg \tau_D$. Here, carrier distributions for constant mobility drift in the reverse direction, and persist for long times. Hence, in contrast to the lifetime case, minority carrier injection may induce the depletion of majority carriers.

The depletion region capacitance of a uniformly doped lifetime diode at full depletion may be expressed in terms of the dielectric constants as

$$C_d = \frac{\varepsilon_r\varepsilon_0 A}{d} \tag{4}$$

where A is the active diode area and d the depletion width. The capacitance arises as a result of charge variation within a reverse-biased space charge region of a semiconductor junction device. This in turn results from applying to the device a d.c. voltage onto which a small amplitude a.c. voltage is modulated [7, 8]. In this situation, the effective carrier concentration is evaluated from

$$C_d^{-2} = \frac{2}{e\varepsilon_r\varepsilon_0 A^2}\,\frac{1}{N_{\text{eff}}}\,V_d \tag{5}$$

where V_d is the full depletion voltage. This relation shows that $N_{\text{eff}} \propto V_d\,C_d^2$, which may be simplified to $V_d \propto C_d^{-2}$ for a constant effective carrier concentration, which is the case for uniform doping and is assumed for lifetime material. However, in the relaxation regime full depletion is determined by the width of the maximum resistivity region [6] and $I \propto V_d$ as seen later in equation (7). Because the current is ohmic and is generated in the whole of the depletion region, $d \propto V_d$ and so N_{eff} is not constant. The capacitance becomes a function of temperature since electrons and holes are thermally activated, and so the effective carrier concentration is variable with temperature. Furthermore, since in the relaxation regime different trapping centres respond to different frequencies, the capacitance of relaxation devices is frequency dependent. In consequence, the carrier concentration measured in this way is variable with the measurement frequency.

The charge that is collected by a semiconductor diode detector is dependent upon the number of e–h pairs that are created in the detector by the incident charged particle. The e–h pairs are a consequence of the Coulomb interaction of the charged particle and the electrons of the host material. The amount of charge that is measured is determined by the proportion of the total distance between the electrodes that the electrons and holes will traverse in the electric field across the device. Therefore, charge collection efficiency (CCE) depends on the capture mean free path of charge carriers [9, 10]. Charge capture reduces the measured charge and hence decreases the signal-to-noise ratio, and also causes a spread in the charge. The detector resolution is evaluated from the pulse amplitude spectrum as

$$R = \frac{2.35\sigma}{H_0} \tag{6}$$

where σ is the standard deviation and H_0 is the centroid of the peak. Both σ and H_0 can be extracted from a Gaussian fit to the data. The dependence of the charge collected on the mean free path means that to achieve high values of CCE, the capture times for compensating levels must be sufficiently long, or the capture cross sections sufficiently small.

2. The devices

The devices are two square (10 mm × 10 mm) p–i–n photodiodes fabricated from high resistivity (400 Ω cm) n-type silicon. Pre-irradiation measurements have shown the two diodes to be quite similar. We denote the first unirradiated diode pin0 and note that it has zero fluence, $n0$. We have measured the active substrate thickness by the capacitance–voltage technique and found it to be $\sim 240\ \mu$m [6] in both devices. The photodiodes were then irradiated by 1 MeV neutrons at the Rutherford Appleton Laboratory (RAL). Device pin0 was irradiated to an initial fluence of $n1 = 3.39 \times 10^{13}$ n cm^{-2} and then denoted pin1. A subsequent dose of 4.9×10^{13} n cm^{-2} was carried out some months later to give a total of $n2 = 8.29 \times 10^{13}$ n cm^{-2}, after which the device was denoted pin2. The second photodiode was irradiated to a fluence of $n3 = 2.5 \times 10^{14}$ n cm^{-2} and then denoted pin3. The devices pin0, pin1 and pin2 are the same photodiode but with different doses, while pin3 is a different photodiode. Current–voltage (I–V), capacitance–voltage (C–V) and charge collection efficiency (CCE) measurements have been performed both prior to irradiation and soon after on all four devices. In between measurements and irradiations, the detectors were stored at temperatures below zero to reduce possible reverse annealing at elevated temperatures.

3. Experiments

The current–voltage measurements were performed at 300 K. The data were taken both in forward bias and in reverse bias. For isolation from the surroundings, the device was placed in the dark and under vacuum in a chamber-type cryostat. Further isolation was achieved by mounting the diodes onto a metal plate resting on a set of small Teflon balls. All data were acquired with a remotely controlled pA meter with a d.c. voltage source. The sample was biased up to 100 V in either direction, and current limited to 10 mA. Logarithmic plots of current against bias voltage were generated and plotted together with a line corresponding to the maximum resistivity which is evaluated from the relation

$$I = \frac{A}{\rho_{\max}L_d}\,V_d \tag{7}$$

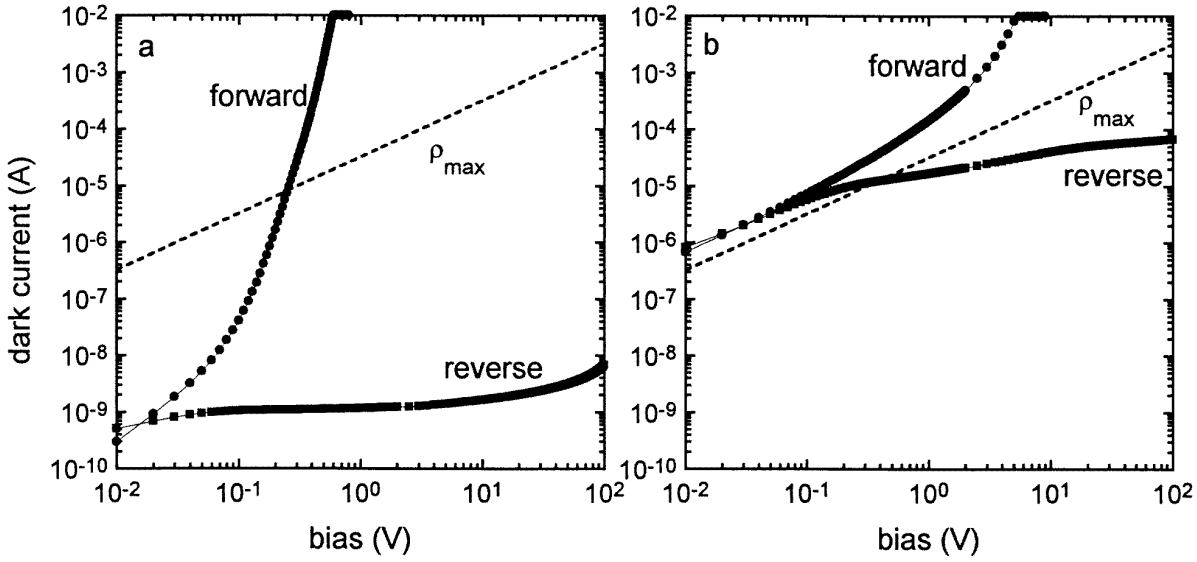

Figure 1. The I–V characteristic (a) before irradiation for pin0, and (b) after irradiation for pin1 at 300 K. In the first situation the characteristic is more 'diode-like', while in the latter case the current approaches the $\rho_{\max}$ line, both in the reverse and in the forward bias directions.

where $\rho_{\max}$ is deduced from equation (2) and L_d is the active thickness of the device. Here, we assume that the device is not fully depleted but that the undepleted layer is of low resistivity. Current–voltage measurements were also carried out over a range of temperatures from 200 K to 350 K. From a temperature profile of the I–V characteristic at reverse bias, a set of Arrhenius plots were generated at each voltage. A linear fitting to these data was used to determine the activation energy of the material at these voltages. A variation of the activation energy with reverse bias voltage was thus generated.

Capacitance–voltage data were acquired manually over a range of temperatures and frequencies with a low-frequency capacitance bridge. The temperature data (C–V–T) were recorded at 10 kHz in the temperature range 200–350 K. The frequency data (C–V–f) were acquired at 300 K in the frequency range 10–200 kHz. Semi-logarithmic data of the C–V variation with temperature were generated that showed the point at which the diode just becomes depleted. This occurs when the capacitance of the device has reached a minimum. The depletion is determined by the space charge in lifetime material and by the maximum resistivity region in the relaxation case. The capacitance falls as $V^{-1/2}$ towards C_d and a linear fit to these data intersects a linear fit to the minimum capacitance data. This intersection gives the depletion voltage V_d. A similar procedure was followed for the C–V variation with frequency. Data were also taken from 20 Hz to 1 MHz in the temperature range 280 to 330 K. A profile of the variation of the capacitance with frequency over a range of temperatures was thus generated and the data were fitted to the Debye relation [11] of the form

$$C = C_{hf} + \frac{C_{lf}}{1 + \omega^2\tau^2} \tag{8}$$

where C_{hf} and C_{lf} are the high- and low-frequency capacitances, respectively, ω is given in terms of the characteristic frequency f as $\omega = 2\pi f$, and τ is the characteristic time constant. We fit the data over a range of temperatures to extract a set of time constants which yield defect parameters of a trapping centre that may be active in that temperature range.

The charge collection measurements were performed on all devices with the aid of an Americium-241 alpha source, of energy 4.52 MeV. The α-particles were made to be incident on to the top (n^+) contact of the reverse biased device, and the resulting signal measured. Of course, after type inversion the top contact has become p^+, which is the case in pin2 and pin3. The source was collimated to a circular aperture of diameter 0.8 mm. The charge signals were processed by a charge-sensitive preamplifier with a rise time of 4 μs, and a shaping amplifier with a shaping time of 0.5 μs for noise reduction purposes. Data were acquired with a multi-channel analyser that has been interfaced with a personal computer for automatic readings. The data were recorded at 300 K and over a period of two thousand seconds for several bias voltages both below and above full depletion. A normally distributed pulse amplitude spectrum was generated and the data were then fitted to a Gaussian distribution. The fitting yields the peak centroid and the peak width which are used to evaluate the detector resolution as in equation (6). By calibrating the system to a silicon detector of 100% efficiency, the CCE of the sample detector can be evaluated from the ratio of the centroid energies as

$$\mathrm{CCE} = \frac{H_0(\mathrm{pin})}{H_0\ (\mathrm{Si})} \times 100\% \tag{9}$$

at each voltage, where pin refers to the p–i–n photodiodes after irradiation (that is pin1, pin2 and pin3), and Si to the

silicon detector before irradiation (that is pin0), which is assumed to be of 100% efficiency.

4. Results and discussion

The measurement of the current at 300 K as a function of bias voltage before irradiation has indicated that the photodiodes were 'normal' diodes, with high current flow in the forward direction, but only minimal flow in reverse bias. In both devices the current in forward bias is exponential with an ideality factor $\eta = 1.85$, and reaches the measurement current limit at 0.7 V (figure 1(a) for pin0). The former situation means that the diffusion and recombination currents are comparable. In reverse bias the current starts to saturate at kT/e, and is nearly constant up to $80kT/e$, which indicates the dominance of generation current, as expected for a lifetime device in which n_i is small [12]. At higher reverse voltages, the current begins to increase rapidly, suggesting that the device is approaching breakdown. After the device had been irradiated, the reverse current has increased by three orders of magnitude (figure 1(b) for pin1), and at lower voltages is parallel to the $\rho_{\max}$ line. In forward bias the current is no longer exponential and it reaches the current limit at 5.6 V. In the reverse direction, the diffusion current is not observed, and there is no indication of possible device breakdown at all. It is clear that the current tends to approach the $\rho_{\max}$ line both in reverse bias and in forward bias. This is an indication that the substrate is tending to be high-resistivity material, or that it is acquiring 'relaxation' properties.

The diodes were repeatedly tested at regular periods to determine if there was any current runaway with time—this was not observed at the measurement temperatures, which indicates some form of stability at these temperatures. At high voltages for device pin1, slight current oscillations have been observed at temperatures below 230 K, and device breakdown has been indicated at temperatures beyond 340 K. This indicates that the device operates well as a detector only within this temperature range.

In figure 2 is a plot of the variation of the forward current with different radiation fluences for all devices. As the fluence increases, the voltage at which the diode reaches the current limit increases, with the consequence that the current becomes parallel to the line of maximum resistivity, an indication that the device is becoming ohmic (or that the material is becoming relaxation). In reverse bias a similar behaviour has been observed. Seen in figure 3 for pin1 is the variation of the activation energy of the material with reverse bias voltage. The activation energy is always close to half bandgap, an indication that the Fermi level is pinned near midgap, the location for minimum conductivity. This means that the device has poor conductivity, or that the material is high resistivity. Furthermore, since the dominant mechanism of minority carrier generation is associated with recombination centres near the middle of the energy gap, pinning of the Fermi level at this position suggests that the device is dominated by this type of carrier generation. This is a feature of relaxation devices.

The plot of figure 4 shows the temperature variation of the C–V characteristic at 10 kHz for pin0 (figure 4(a)) and for pin1 (figure 4(b)). In the first case there is no temperature dependence, as expected for a lifetime device. A dependence is observed in the second case up to the full depletion voltage, as expected for a relaxation device. The variation of V_d and N_{eff} with temperature for pin1 is shown in figure 5. The full depletion voltage as a function of temperature is initially constant at low temperatures, but rises steadily beyond 300 K as shown in (a). This situation has been observed by other workers [13, 14] and can be attributed to ionized carriers that increase the space charge at these high temperatures, which is possible since the device is becoming relaxation-like. The peak at room temperature cannot at present be explained. In figure 5(b), the effective carrier concentration is at first constant but rises steadily at higher temperatures. This can be explained up to 320 K similarly as the increase in V_d when T

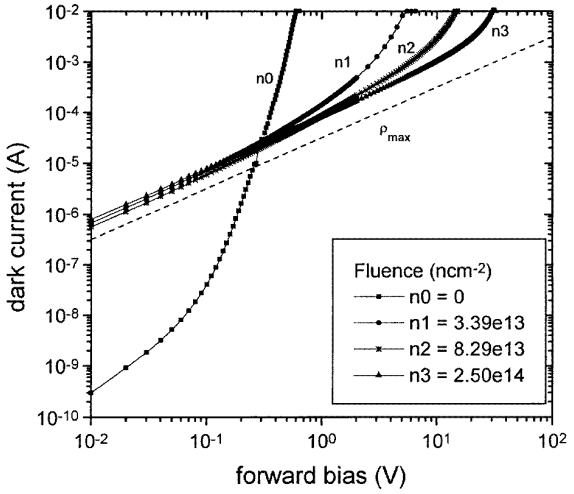

Figure 2. The forward bias I–V characteristic for different fluences at 300 K. The device is becoming more relaxation-like with increasing fluence, as noted by the current following the line of maximum resistivity.

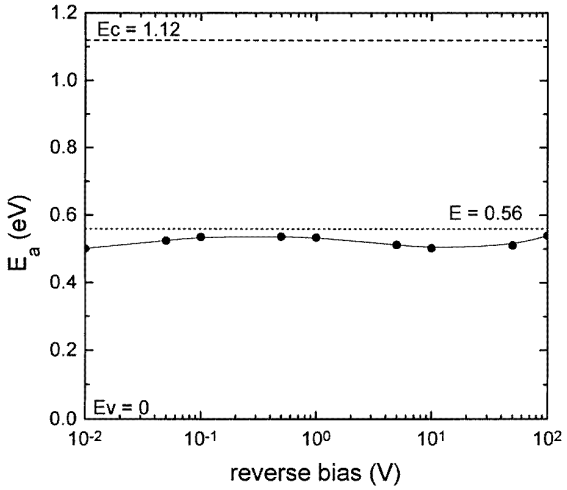

Figure 3. The variation of the material activation energy with voltage for pin1. The activation energy is constantly below midgap, but nearly equal such that the Fermi level is pinned at this position.

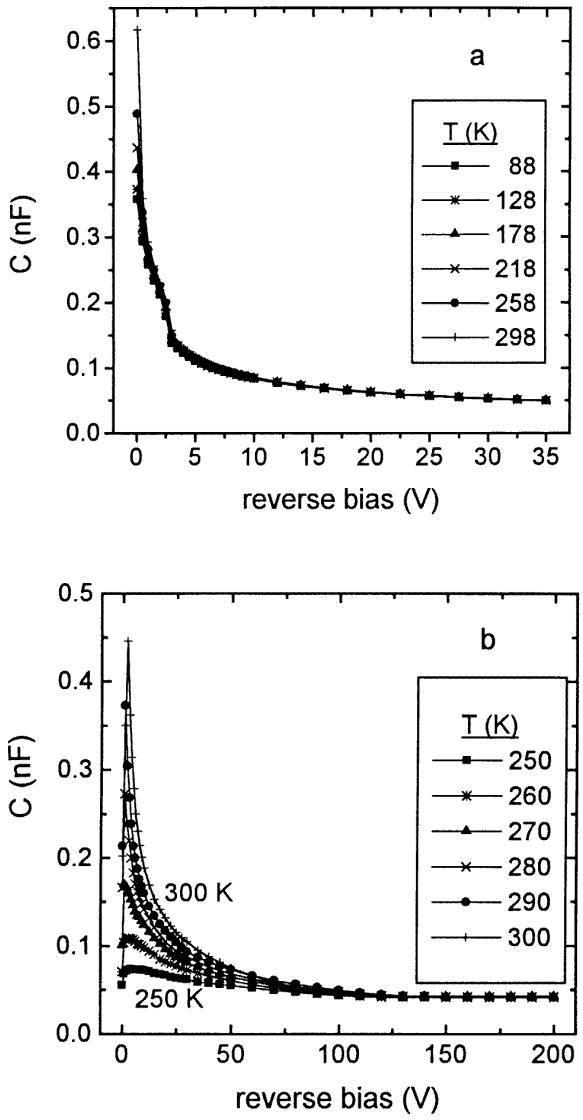

Figure 4. The temperature variation of the $C-V$ characteristic at 10 kHz before irradiation (*a*) and after irradiation (*b*) for pin1.

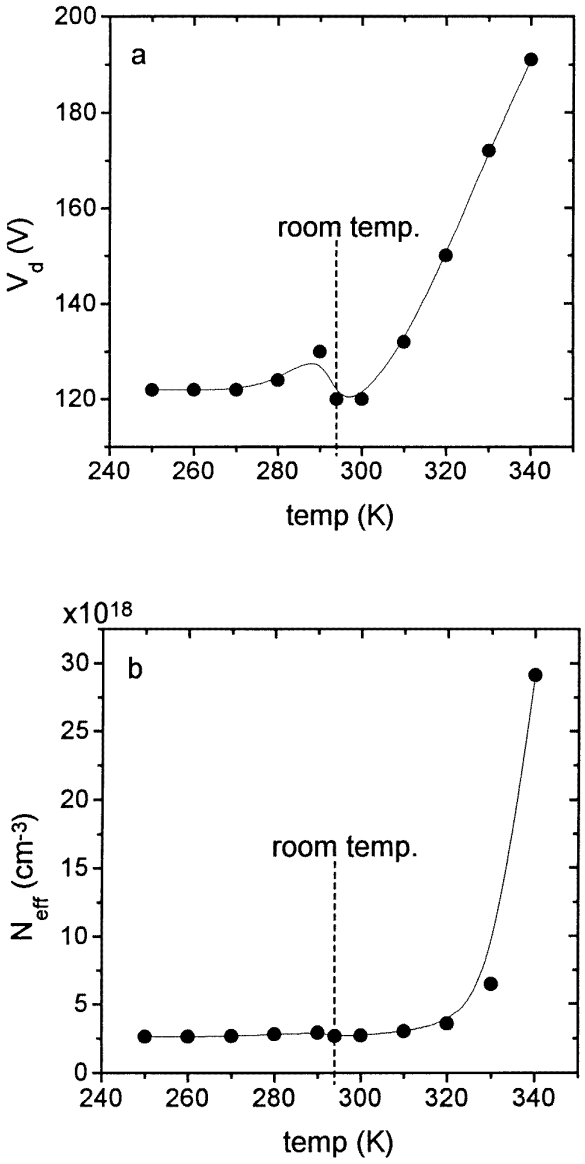

Figure 5. The variation of the full depletion voltage (*a*) and the effective carrier concentration (*b*) with temperature at 10 kHz for pin1. Both are initially constant at low temperatures, but rise steadily beyond room temperature. The peak in the voltage around room temperature is not seen in the plot of N_{eff}.

rises. The sudden increase beyond 320 K is due to impact ionization caused by the inability of the bias voltage to draw out the ionized carriers, and so the increase in N_{eff} results in breakdown. These two effects are features of relaxation devices.

Figure 6(a) is the frequency variation of V_d at 300 K. The depletion voltage falls steadily as frequency rises, in direct contrast to the temperature variation of figure 5(a). The behaviour of the effective carrier concentration seen in figure 6(b) is similarly in the opposite sense to that of figure 5(b). This follows from the fact that for relaxation devices carriers are thermally activated, in which case a relation of the form $\log f \propto -1/T$ holds. This can also be seen for pin2 in figure 7(a), where the capacitance measured at a fixed voltage increases with rising temperature, but falls with increasing frequency. Also, the capacitance is observed to vary considerably at low frequencies but to saturate at higher frequencies. Furthermore, the characteristic frequency increases with increasing temperature, indicating that the diode capacitance is time dependent, another feature of relaxation devices. The data of 330 K have been fitted to the relation of equation (8) in figure 7(b). The fit is fairly reasonable, yielding a time constant $\tau = 3.74$ ms, a high frequency capacitance $C_{hf} = 0.62$ nF and a low frequency capacitance $C_{lf} = 53.95$ nF.

The peak position before irradiation is observed in figure 8(a) for pin0 at the same channel and with the same amplitude for a range of voltages from 50 V to 200 V. After the device has been irradiated, the peaks appear at different (and lower) channels for different bias voltages, as seen in figure 8(b) for pin1. This indicates that charge is

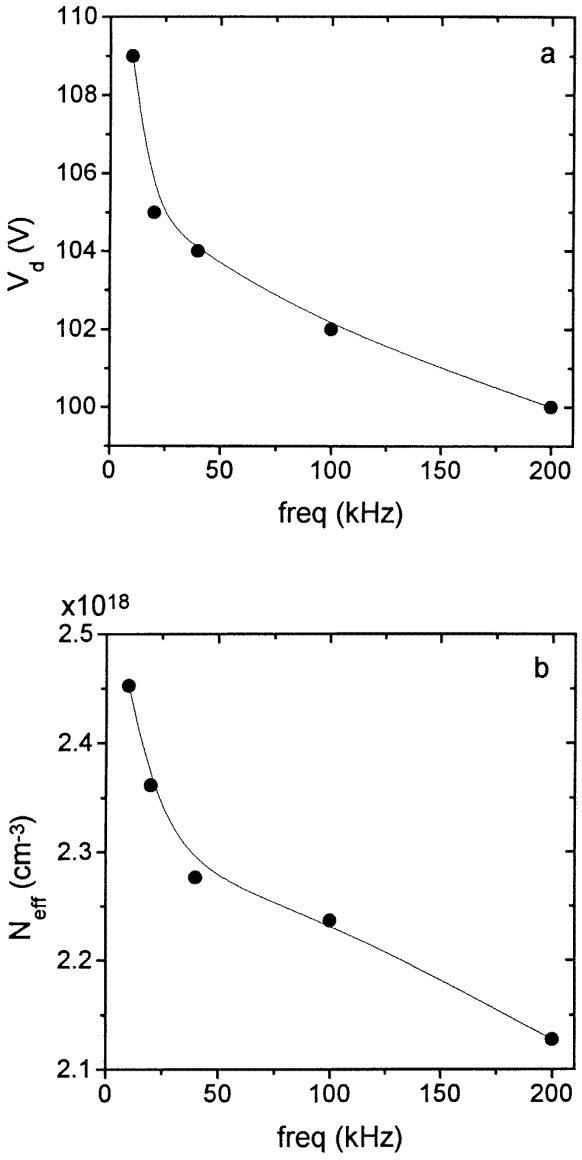

Figure 6. The frequency variation of the full depletion voltage (*a*) and of the effective carrier concentration (*b*) at 300 K for pin1. Both V_d and N_{eff} fall steadily as the frequency rises.

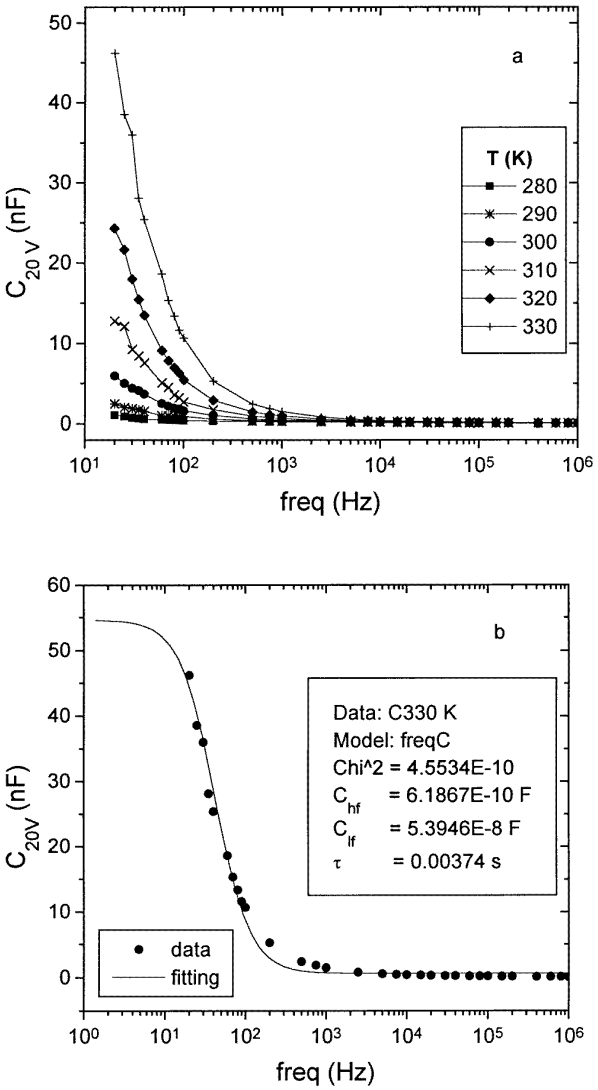

Figure 7. A profile of the *C–f* characteristic over a range of temperatures for pin2 at 20 V at reverse bias. A variation of $\omega\tau$ with temperature is clearly observed in (*a*), while in (*b*) a fitting to the 330 K data yields τ = 3.74 ms.

being trapped before collection on the opposite electrode. Also, no peak was observed below 90 V in reverse bias, suggesting that the device is beginning to type invert and requires a higher voltage for the charge to traverse the p^+ region forming on the front side. The resolution of the device at 10 V has degraded from a pre-irradiation value of 0.17 to a post-irradiation value of 0.5 at low bias to 0.17 at higher voltages. This means that the centroid has shifted to lower channels, which occurs because the charge is being captured before collection.

The diode pin0 has been defined as a detector of 100% collection efficiency prior to irradiation. This is because peaks from a calibration pulse occur at the same channel as those of the diode. Figure 9(a) (which has been derived from figure 8(a)) shows that at zero bias some charge can be 'seen' by the lifetime diode, but that as the bias rises, the CCE quickly increases to saturation. The CCE from the front side of pin1 has degraded somewhat after irradiation, and the device only begins to detect the charge at around 90 V (figure 9(b)). At voltages below 90 V, no alphas are observed from the front side, which indicates possible type inversion from n-type to apparent p-type, as stated above. Furthermore, the efficiency has degraded to below 50% at lower voltages but is seen to increase to a saturation value of 97% as the bias is increased. No alphas have been observed from the front side of the diodes with the higher fluence (that is, pin2 and pin3). It is suggested that these devices have type inverted fully, and that the front side is now p^+. It is therefore normal that no alphas were observed.

5. Conclusions

The *I–V* characteristic is becoming more ohmic with increasing fluence, and the Fermi level remains pinned

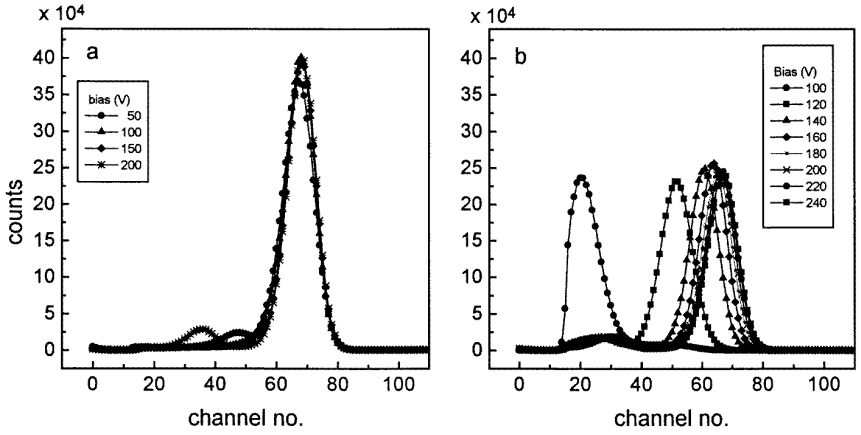

Figure 8. The pulse amplitude spectrum plots (a) before irradiation for pin0 and (*b*) after irradiation for pin1 at 300 K. Except at zero bias, all peaks occur at the same channel in the first case, but at different channels for different voltages in the second case. The pulse amplitude has decreased by nearly a third from the pre-irradiation value.

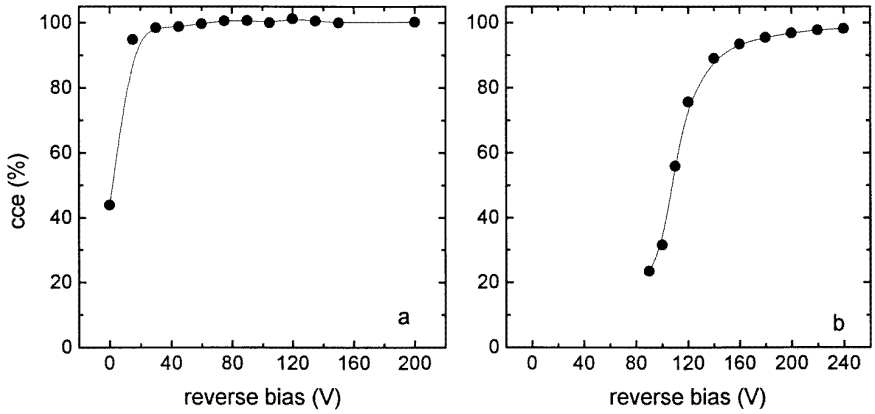

Figure 9. The charge collection efficiency for αs (*a*) before irradiation for pin0 and (*b*) after irradiation for pin1. In (*a*) we note that, except at zero bias, the CCE is 100% at all voltages, while the second case indicates that the CCE has degraded considerably at low voltages but rises to nearly 100% at higher voltages.

near midgap. The irradiated material is clearly acquiring relaxation-like characteristics. The C–V characteristic has become frequency dependent after irradiation, and an increase in V_d and in N_{eff} is occurring at high temperatures, all of which are features of relaxation behaviour. Irradiated silicon is therefore relaxation material. The data need further analysis, however, to better understand the peak in depletion voltage at room temperature.

The CCE experiment indicates a charge collection deficiency at low bias voltages, but only a slight decrease at higher voltages for the device with lowest fluence (pin1). This suggests that the depleted region has begun to move to the back side of the device, a feature which indicates the onset of type inversion. The resolution of detector pin1 has degraded considerably, further indicating that the device has already begun to undergo type inversion. In this material type inversion therefore occurs at fluences below 3×10^{13} n cm^{-2}. This is also confirmed by the fact that no alphas were detected from the front side of pin2 and pin3.

The overall degradation in CCE occurs because the device has been damaged by the irradiation. The damage occurs by the formation of defect levels in the bandgap, which induce relaxation behaviour in the material. It is possible that the defects created may anneal out with rises in temperature, and so the relaxation behaviour may be a temporary effect.

Acknowledgments

The first author wishes to thank Z Li and A Chillingarov, the former for introduction to the silicon literature, and the latter for useful discussions.

References

[1] Queisser H J 1972 *Solid State Devices Conf. Ser.* no 15 p 145
[2] van Roosbroeck W 1972 *Phys. Rev. Lett.* **28** 1120
[3] Haegel N M 1991 *Appl. Phys.* A **53** 1
[4] Zdansky K, Jones B K, Santana J and Sloan T 1996 *J. Appl. Phys.* **79** 3611
[5] Jones B K, Santana J, Sloan T and Zdansky K 1996 *GaAs and Related Compounds* eds P G Pelfer, J Ludwig, K Runge and H S Rupprecht (Singapore: World Scientific) p 73

[6] Jones B K, Santana J and McPherson M 1996 *Semi-insulating GaAs or Silicon, 4th Int. Workshop on GaAs and Related Compounds (3–6 June 1996, Aberfoyle)* to be published in *Nucl. Inst. Meth.* **A394**
[7] Schroder D K 1990 *Semiconductor Material and Device Characterization* (New York: Wiley)
[8] Blood P and Orton J W 1992 *The Electrical Characterization of Semiconductors: Majority Carriers and Electron States* ed N H Marsh (London: Academic)
[9] Knoll G F 1989 *Radiation Detection and Measurement* 2nd edn (New York: Wiley)
[10] Berwick K, Brozel M R, Buttar C M, Cowperthwaite M and Hou Y 1993 *Mater. Res. Soc. Symp. Proc.* **302** 363
[11] Daniel V V 1967 *Dielectric Relaxation* (London: Academic)
[12] Sze S M 1969 *Physics of Semiconductor Devices* (New York: Wiley)
[13] Mathews J A J, Berdusis P, Schuler J, Sadrozinski H, O'Shaughnessy K, Palounek A and Ziock H 1996 *Nucl. Inst. Meth.* **A381** 338
[14] Beattie L, Chillingarov A, Ratoff P and Sloan T 1997 *Rose Technical Note* **97/4**